

# Processes of radionuclide enrichment in sediments and ground waters of Mont Vully (Canton Fribourg, Switzerland)

Autor(en): **Schott, Bernd / Wiegand, Jens**

Objektyp: **Article**

Zeitschrift: **Eclogae Geologicae Helvetiae**

Band (Jahr): **96 (2003)**

Heft 1

PDF erstellt am: **28.06.2024**

Persistenter Link: <https://doi.org/10.5169/seals-169009>

## **Nutzungsbedingungen**

Die ETH-Bibliothek ist Anbieterin der digitalisierten Zeitschriften. Sie besitzt keine Urheberrechte an den Inhalten der Zeitschriften. Die Rechte liegen in der Regel bei den Herausgebern. Die auf der Plattform e-periodica veröffentlichten Dokumente stehen für nicht-kommerzielle Zwecke in Lehre und Forschung sowie für die private Nutzung frei zur Verfügung. Einzelne Dateien oder Ausdrucke aus diesem Angebot können zusammen mit diesen Nutzungsbedingungen und den korrekten Herkunftsbezeichnungen weitergegeben werden. Das Veröffentlichen von Bildern in Print- und Online-Publikationen ist nur mit vorheriger Genehmigung der Rechteinhaber erlaubt. Die systematische Speicherung von Teilen des elektronischen Angebots auf anderen Servern bedarf ebenfalls des schriftlichen Einverständnisses der Rechteinhaber.

## **Haftungsausschluss**

Alle Angaben erfolgen ohne Gewähr für Vollständigkeit oder Richtigkeit. Es wird keine Haftung übernommen für Schäden durch die Verwendung von Informationen aus diesem Online-Angebot oder durch das Fehlen von Informationen. Dies gilt auch für Inhalte Dritter, die über dieses Angebot zugänglich sind.

# Processes of radionuclide enrichment in sediments and ground waters of Mont Vully (Canton Fribourg, Switzerland)

BERND SCHOTT & JENS WIEGAND

*Key words:* Radon, radium, uranium, radioactive disequilibrium, radionuclide mobility, molasse sediments, ground water

## ZUSAMMENFASSUNG

Während einer Erhebung der Radonkonzentrationen ( $^{222}\text{Rn}$ ) in Grundwässern des Schweizer Molassebeckens durch das Bundesamt für Gesundheit wurden erhöhte Konzentrationen am Mont Vully (Kanton Freiburg) gemessen. Teilweise liegen die  $^{222}\text{Rn}$ -Konzentrationen um ein 10faches über denen benachbarter Grundwasserleiter, trotz vergleichbarer Geologie. Die vorliegende Studie befasst sich mit Ursachen und Prozessen, die zu dieser Erhöhung führen. Sowohl Wasserproben von 25 Trinkwasserfassungen als auch Sedimentproben von Aufschlüssen der Oberen Meeresmolasse wurden dazu genommen. Insbesondere in den Sedimentproben treten deutliche radioaktive Ungleichgewichte innerhalb der  $^{238}\text{U}$ -Zerfallsreihe auf, die ihre Ursache in einer mehrphasigen Radionuklid-Mobilisierung und -Verlagerung haben. Eine erste Anreicherung von Uran fand synsedimentär an organischem Material (Knochen) statt. Durch die Zersetzung der organischen Substanz bildete sich ein reduzierendes Milieu, wodurch im Wasser gelöstes Uran ausfiel. Seit dieser primären Anreicherung sind  $^{226}\text{Ra}$ , aber auch Fe und Mn, unter reduzierenden Bedingungen, wie sie für gewöhnlich im Stauwasserbereich herrschen, mobilisiert und unter oxidierenden Bedingungen nahe des Grundwasserspiegels immobilisiert worden. Besonders entlang von bevorzugten Wasserwegsamkeiten (Störungen und Klüfte) bildeten sich Fe- und Mn-Hydroxide, die effizient Radium aus dem Wasser adsorbieren. Die exponierte Lokation des  $^{226}\text{Ra}$  an den Fe- und Mn-Hydroxiden führt zu einem hohen  $^{222}\text{Rn}$ -Emissionskoeffizienten sowie zu hohen  $^{222}\text{Rn}$ -Konzentrationen im Grundwasser und die gute Wasserleitfähigkeit ermöglicht große  $^{222}\text{Rn}$ -Migrationsweiten.

## ABSTRACT

During a survey of radon concentrations ( $^{222}\text{Rn}$ ) in ground waters of the Swiss molasse basin carried out by the Swiss Public Health Office, high concentrations were observed at Mt Vully, which is a small hill. The present study was conducted to elucidate the processes leading to  $^{222}\text{Rn}$  concentrations, which were several times higher than those of neighbouring aquifers. Ground waters from 25 water catchments and sediments of the outcropping Upper Marine Molasse were sampled. These are characterised by radioactive disequilibria within the  $^{238}\text{U}$  decay series, most pronounced in the sediments, which reveal a complex history of radionuclide mobility and displacement: A first enrichment in radionuclides occurred in early diagenetic times, when uranium precipitated on organic materials (bones) producing a reducing halo during degradation. Since this time, Fe, Mn and  $^{226}\text{Ra}$  have been mobilised under local reducing conditions and transported with the ground water stream. Especially along permeable zones like faults and joints, Fe and Mn hydroxides are precipitated under oxidising conditions, and  $^{226}\text{Ra}$  is adsorbed on the hydroxides. The high  $^{222}\text{Rn}$  concentrations in the ground waters are due to the high  $^{222}\text{Rn}$  emanation coefficients of faults and joints mineralised with Fe and Mn hydroxides, which act as preferential ground water pathways.

## 1. Introduction

Radon ( $^{222}\text{Rn}$ ) has been recognised as the predominant source of potential adverse health effects from exposure to natural radioactivity from pathways including drinking water, other foods or in indoor air (UNSCEAR 2000).  $^{222}\text{Rn}$  is a naturally occurring alpha-emitting noble gas with a half-life of 3.8 days, and is present in ground waters in easily measurable concentrations.

A survey of  $^{222}\text{Rn}$  in ground and spring waters from the Swiss cantons Fribourg and Vaud, hosted by the Swiss Federal Office of Public Health, reported  $^{222}\text{Rn}$  concentrations

with a median value of 9 Bq/l (Völkle & Gobet 1997). During a subsequent ground water survey conducted in a small-sized Tertiary molasse aquifer at Mont Vully (Canton Fribourg), unusually high concentrations of  $^{222}\text{Rn}$ , exceeding 100 Bq/l, were detected by Surbeck (pers. communication). However, the Mt. Vully aquifer shows a similar hydrogeological setting as the surrounding aquifers. The observed concentrations are within the regulatory guidelines for liquid foods (limit value: 1 Bq/l for the total of all non-gaseous alpha-emitters; Eidgenössisches Departement des Innern

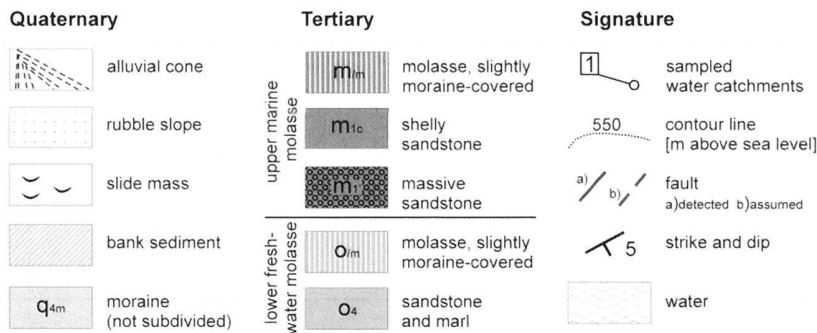
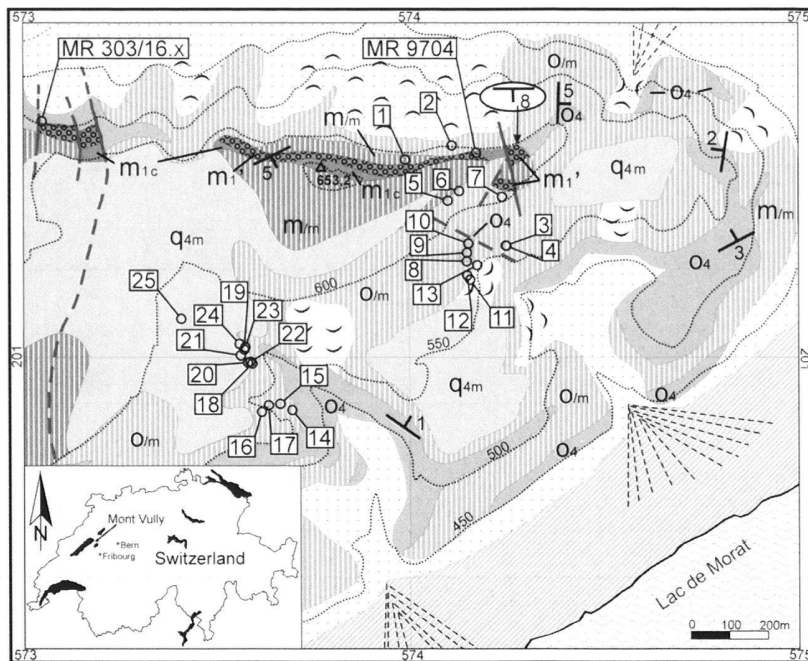


Fig. 1. Simplified geological map of the Mt. Vully with location of sediment samples and water catchments (geology after Becker 1973 and Becker & Ramseyer 1972; coordinates are the rectangular coordinates centred in the capital Bern).

1995), but nevertheless this study was conducted to clarify the reasons for the higher  $^{222}\text{Rn}$  concentrations in the ground waters of Mt. Vully. In the course of this study different pronounced radioactive disequilibria within the  $^{238}\text{U}$  decay series were observed, which reveal a multi-stage chronicle of radionuclide displacement. In the following, the deduced processes of radionuclide mobility and enrichment will be presented and discussed in detail.

## 2. Geology and hydrogeology of Mt. Vully

The study site represents the eastern part of a small hill named "Mont Vully". This hill is located in western Switzerland NE of Fribourg (Fig. 1), and lies within the Swiss Molasse Basin. The asymmetric basin, which is filled with up to 6000 m thick Tertiary sediments, stretches approx. 300 km in SW – NE direction. To the NW the basin is bordered by the folded Jura mountains, and to the SE by the Alps. Since Studer (1853) the Oligocene and Miocene sediments of the molasse basin are

subdivided into four groups (from bottom to top): "Lower Marine Molasse – Lower Freshwater Molasse – Upper Marine Molasse – Upper Freshwater Molasse".

### 2.1 Geologic setting

The WSW - ENE striking hill of Mt. Vully is situated between the lakes "Lac de Morat" and "Lac de Neuchâtel" (Fig. 1). The hill reaches an altitude of 653 m, and lies well above the level of the two adjacent lakes, which are situated at an altitude of 430 m. The bedrock of Mt. Vully comprises mainly late Oligocene to early Miocene sediments of the Lower Freshwater Molasse (USM), and to a lesser extent early to middle Miocene Upper Marine Molasse (OMM). The deposition of the terrestrial sediments took place in several cycles (Ramseyer 1952). Each cycle starts with a partly calcareous sandstone, getting more fine-grained towards the top. It ends with marly sediments, which are wedging out frequently. Only the last cycle has a well extended marl layer with a thickness of ap-

prox. 6 m. This layer is of great hydraulic importance for the Mt. Vully, and marks the border to the overlying OMM (Ramseyer 1952). However, Homewood & Matter (1980) placed the border between USM and OMM approx. 5 to 10 meters higher. This 5 to 10 m thick transition zone between USM and OMM represents the region of interest for the study, which is based on the findings of Schott (1998). The transition zone is built up by deltaic channel deposits, which consist of trough and tabular cross-bedded sandstones with frequently interbedded clay pebbles of lagoonal, marsh and floodplain facies (Homewood & Matter 1980). The lower beds of partly glauconitic sandstones are characterised by interbedded drift wood, plant remains and mammal bones. These fossils are frequently encrusted by precipitations of Fe and Mn hydroxides.

After Homewood & Matter (1980) the OMM sequence starts with a basal conglomerate, which represents the lowest horizon of extra formational pebbles. Following the conglomerate, an approx. 15 m thick cross-bedded glauconitic sandstone layer with sporadically marl lentils had been developed. On the top of the sandstone, a calcareous shell sandstone succession with interbedded limestones finishes the stratigraphic sequence of the molasse sediments at Mt. Vully. Frequently, the molasse sediments are covered by Quaternary deposits, like Würmian moraine deposits, rubble slope and slide masses (Ramseyer 1952; Fig. 1).

From the regional tectonics, the hill of Mt. Vully represents a relief inversion (Ramseyer 1952). A very weak developed structural syncline with flanks dipping no more than a few degrees – the so-called Mt. Vully syncline – strikes WSW - ENE through the central part of the hill. The axis dips slightly to the NE with approx. 2 – 3° (Ramseyer 1952). Another important tectonic element is the S-N striking Sur-le-Mont fault, which separates Mt. Vully into two tectonic blocks (Fig. 1, at the western rim). In comparison to the eastern block, the western part is lowered by about 80 m (Ramseyer 1952).

## 2.2 Hydrogeology

The hydrogeology of the molasse basin is complex due to frequent changes in facies and cementation. A review of the hydrogeology of the whole basin is given by Keller (1992). Following Keller, the USM strata act most often as an aquitard, and the OMM as an aquifer. The region of the folded molasse is a fractured aquifer rather than a porous aquifer.

At Mt. Vully, the calcareous and shelly sandstones of the OMM form a fractured aquifer, which feeds numerous drinking water catchments around the hill (Fig. 1). Meteoric water infiltrates over an area not larger than 2 – 3 km<sup>2</sup>. The aquifer is limited by the underlying impermeable marly beds of the USM. Therefore, several strata springs are located along the borderline between USM and OMM. Other springs follow the Sur-le-Mont fault, which is an important N – S striking structural drainage element for the central part of Mt. Vully. Under a mean annual precipitation of 940 mm, the recharge rate reaches values of around 365 mm/a (Geolina 1993).

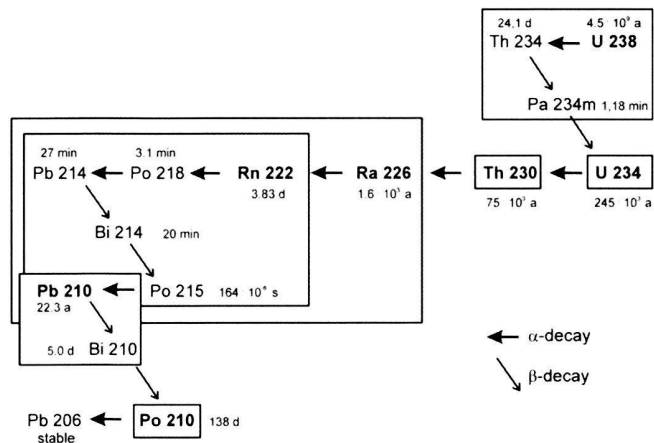


Fig. 2. <sup>238</sup>U decay series (minor decay paths have been omitted) (after Surbeck 1995).

## 2.3 The <sup>238</sup>U decay series

Apart from <sup>40</sup>K, the most prominent natural radionuclides found in rocks, sediments and ground waters are from the <sup>238</sup>U and <sup>232</sup>Th decay series (Osmond & Ivanovich 1992). This study focus on radionuclides from the <sup>238</sup>U series, mainly on <sup>238</sup>U, <sup>234</sup>U, <sup>226</sup>Ra and <sup>222</sup>Rn. While <sup>222</sup>Rn is a short-lived, gaseous radionuclide, the other three nuclides are long-living, non-gaseous precursor of <sup>222</sup>Rn (Fig. 2). Fig. 2 gives information about the kind of decay and the half-lives. Furthermore, the decay series is subdivided into groups indicated by frames. The groups comprise a long-lived mother-nuclide together with her short-living decay-products. Frequently, the radionuclides of a group are in radioactive equilibrium within rocks, sediments and soils. In contrast to that, the different geochemical behaviour of the non-gaseous radionuclides result in radioactive disequilibrium within ground and surface waters.

## 3. Materials and methods

### 3.1 Sample collection of sediments and ground water

The boundary between USM and OMM is well exposed at the old outcrop “military road” where sediment sample MR 9704 was taken. The outcrop, described by Homewood & Matter (1980), is situated north of the summit of the hill (altitude: 620 – 640 m; co-ordinates: 574.2 / 201.5 to 573.7 / 201.5, Fig. 1). Further samples (MR 303/16.x) were collected at the northern end of the Sur-le-Mont fault (Fig. 1). Samples were selected visually (grain size, colour) and radiometrically by an α/β-probe, which measures α- and β-decays simultaneous. Beside the normally green-grey coloured sediments, samples were collected from markedly red or darkly coloured zones (Fe or Mn hydroxides), and from regions with a significantly higher α- and β-activity together with surrounding ordinary sediments.

catchment	ld m	lt m	31.3.1998		5.5.1998		catchment	ld m	lt m	31.3.1998		5.5.1998	
			<sup>222</sup> Rn Bq/l	d l/min	<sup>222</sup> Rn Bq/l	d l/min				<sup>222</sup> Rn [Bq/l]	d l/min	<sup>222</sup> Rn [Bq/l]	d l/min
1	-	-	95	40	97	42	14	10	-	32	8	33	10
2	-	0.5	68	4.5	69	5	15	50	-	55	1	17	1
3	-	1	85	6.5	79	8	16	20	70	26	6	16	11
4	-	1	61	9	53	10	17	10	70	16	6	29	6
5	95	-	10	3	5.7	4	18	40	-	38	1	30	1
6	95	-	9.4	27	11	27	19	40	-	35	1	38	1.5
7	95	-	6.1	3	6.5	3.5	20	40	-	27	4	26	5
8	25	-	42	5	26	5	21	70	30	36	6	35	8
9	7	-	8.8	2.5	10	3	22	30	30	41	0.5	46	1
10	25	-	105	9	103	11	23	10	30	58	2	54	3
11	15	-	23	24	17	24	24	40	30	42	2	39	3
12	30	-	36	1	32	1	25	10	-	40	4	39	4
13	30	-	42	2	38	2							

Tab. 1. Discharge rate and <sup>222</sup>Rn concentrations (1  $\sigma$  error: 8% for < 10 Bq/l, 4% for > 10 Bq/l) of the sampled water catchments (ld = length of drainage pipe; lt = length of transport pipe; d = discharge).

Some investigations at sites additional to the main working area (= eastern block of Mt. Vully) were done in a recently excavated large loam pit named "Les Dailles" (samples W...), which lies 9 km south of Mt. Vully, and exposes a sequence of the USM (co-ordinates 574.3 / 192.4). The strata is build up by mud- and marlstones with intercalated thin layers of sandstone. This outcrop has the advantage of giving access to unaltered rock samples under nearly recent aquifer and aquitard conditions. These sediments were active aquifers and aquitards until the pit was excavated. Such samples are not available at Mt. Vully.

Twenty-five water catchments (i.e. wells, which collect ground water using drainage pipes) serving the public water supply of the municipality Bas-Vully (Fribourg) were sampled (Tab. 1). Unfortunately, it was not possible to consider the water catchments along the Sur-le-Mont-fault. Six manholes (multiple-catchment systems), in which ground waters from 2 – 7 water catchments flow together, and two individually accessible water catchments (1 and 2) were investigated. The water catchments collect water from closely defined sources (catchments 1 – 4), or via 7 – 95 m long drainage pipes (catchments 5 – 25) (Tab. 1). The simplified geological map (Fig. 1) shows the position of the water catchments (1 – 4), and the locations of the beginning of the drainage pipes (catchments 5 – 25). The water catchments 1 – 17 collect water from a catchment area not larger than 0.4 km<sup>2</sup> (Geolina 1993). The catchment area of the other examined water catchments is unknown, but it is probably of a similar extent.

Water samples of all 25 water catchments were taken on the same day. Vessels (vials and bottles) were filled brim-full directly at the afflux of the catchment into the manhole (exception catchment 2 where only a spigot is available). Two 40 ml radon-tight glass vials served for the <sup>222</sup>Rn determination. The full vials were capped under the water jet. Subsequent to the sampling, discharge, electrical conductivity, pH and temperature were measured at each catchment.

Because of the greater probability of short term variability compared to the non-gaseous radionuclides, water samples for the determination of <sup>222</sup>Rn were taken and measured twice (Tab. 1). The first sampling was conducted on 31 March 1998 (mc 1 in Fig. 4), the second followed after a rainy period on 5 May 1998 (mc 2 in Fig. 4).

### 3.2 Sample analysis

The sediment samples were analysed as follows: Pressed pills were measured by X-ray analysis for main and trace element determination. Among the radionuclides, members of the <sup>238</sup>U decay series (<sup>234</sup>Th, <sup>226</sup>Ra, <sup>210</sup>Pb), and the <sup>232</sup>Th decay series (<sup>228</sup>Ac, <sup>212</sup>Pb, <sup>208</sup>Tl) were analysed by  $\gamma$ -spectroscopy. Assuming that there was no geochemical process of loss or enrichment of uranium or thorium isotopes during the last 100 days within the sediments (4 half-lives of <sup>234</sup>Th), the determined <sup>234</sup>Th concentrations can be viewed as <sup>238</sup>U concentrations (Fig. 2). This has been assumed in the following descriptions. The air-dried samples were sealed in gas-tight boxes to prevent loss of <sup>222</sup>Rn. Samples were measured by using a Low-Level High-Purity Germanium (HPGe) well detector or a n-type Low-Level HPGe detector (Surbeck 1991). To get information about the <sup>222</sup>Rn availability of the sediments, the <sup>222</sup>Rn emanation coefficient was determined, by crushing, drying and sealing samples in <sup>222</sup>Rn-tight emanation chambers. The <sup>222</sup>Rn emanation coefficient results from the ratio of the released (emanated) <sup>222</sup>Rn, and the <sup>226</sup>Ra concentration of the sample. The samples were water saturated to enhance the emanation rate (Tanner 1980). After a standby time of approx. 14 days sufficient <sup>222</sup>Rn was formed by the decay of <sup>226</sup>Ra and an air sample of the chamber was transferred into a Lucas cell for measurement (Schmidt & Wiegand 1998). The detection limit of this method is 0.1 (Bq/kg)/(Bq/kg) respectively 10 %.

The water samples were analysed for main cations (Na, K, Mg, Ca, Sr, Ba, Mn, Fe) and anions (SO<sub>4</sub>, PO<sub>4</sub>, NO<sub>3</sub>, HCO<sub>3</sub>, Cl) as well as <sup>238</sup>U, <sup>234</sup>U, <sup>226</sup>Ra and <sup>222</sup>Rn. For the determination of <sup>238</sup>U, <sup>234</sup>U and <sup>222</sup>Rn liquid scintillation alpha spectroscopy was applied. The detection limit of this method is 50 mBq/l. The <sup>226</sup>Ra activity concentration was measured using a method from the Swiss Federal Office of Public Health for the detection of radium in low-barium drinking water – using a polyamide slab (400 mm<sup>2</sup> surface) coated on both sides with MnO<sub>2</sub> which adsorbs radium (Surbeck 1997). The slabs are measured by alpha spectroscopy. The detection limit of this method is 5 mBq/l (Surbeck 1995).

Tab. 2. Radionuclide concentrations ( $2\sigma$  error) of the sandstones (mean values) and selected samples from Mt. Vully (MR samples) and Les Dailles (W samples), <sup>(1)</sup> data from Surbeck, pers. communication).

sample	description	<sup>238</sup> U [Bq/kg]	<sup>226</sup> Ra [Bq/kg]	<sup>210</sup> Pb [Bq/kg]
sandstone (n=8)	background	33 +/- 9	34 +/- 17	42 +/- 6
W 93/1 <sup>(1)</sup>	bone fragment	5800 +/- 2200	6500 +/- 2100	3800 +/- 200
W 93/2 <sup>(1)</sup>	2mm-layer around W93/1	130 +/- 64	270 +/- 90	380 +/- 40
MR 303/16.4.1	outer part of bone	2370 +/- 140	2800 +/- 300	2130 +/- 130
MR 303/16.4.2	central part of bone	1920 +/- 90	1680 +/- 190	1190 +/- 80
MR 303/16.7	bone marrow cavity	600 +/- 50	1440 +/- 130	550 +/- 50
MR 9704	bone fragment	38700 +/- 800	25000 +/- 2000	11300 +/- 300
W 93/4 <sup>(1)</sup>	green-grey, soft	1300 +/- 200	370 +/- 250	300 +/- 150
W 93/5 <sup>(1)</sup>	green-grey, hard	2000 +/- 300	800 +/- 30	790 +/- 130
W 93/6 <sup>(1)</sup>	green-grey, partly black	< 65	6400 +/- 200	2600 +/- 130
W 93/6.1 <sup>(1)</sup>	black parts of W 93/6	< 300	65300 +/- 1400	23800 +/- 600

#### 4. <sup>238</sup>U series disequilibria in sediments

Tab. 2 gives radionuclide concentrations of the <sup>238</sup>U series of some radionuclide enriched sediments and fossils of the working area. The concentrations of the <sup>232</sup>Th series are not shown and not discussed, because no significant radioactive disequilibrium within this series was observed. The “background concentration” of the sandstone is approx. 35 Bq/kg for the <sup>238</sup>U series (Tab. 2, “sandstone”), and 23 Bq/kg for the <sup>232</sup>Th series (Schott 1998).

##### 4.1 Mt. Vully and Les Dailles

The first group of individual samples given in Tab. 2 (W 93/1 – MR 9704) are characterised by very high radionuclide concentrations. Those samples are bone fragments with Ca and P concentrations of approx. 25 wt-%, resp. 10 wt-% (Schott 1998). The <sup>238</sup>U concentrations vary between 600 and 38700 Bq/kg, which is equal to approx. 50 – 3000 ppm U under radioactive equilibrium conditions. Bones *in vivo* have very low average U concentrations of less than 0.1 ppm (Schwarz & Blackwell 1992), indicating that the observed <sup>238</sup>U concentrations cannot be traced back to a high U content of bones, but to a subsequent enrichment.

The samples W 93/1 and W 93/2 (Tab. 2), sampled and analysed by Surbeck (pers. communication), show that the enrichment of radionuclides is limited to the bone fragments. Even within distances of 2 mm, the <sup>238</sup>U concentrations are close to the background. To get an idea of the U distribution within the bone fragments, the sample MR 303/16 was fractionated into three sub samples (Tab. 2: MR 303/16.4.1, 16.4.2, 16.7), which represent a section through a bone. Similar to the results of Badone & Farquhar (1982), the <sup>238</sup>U concentrations decrease approaching the central parts of the bone. The relatively low <sup>238</sup>U concentration of the marrow cavity (MR 303/16.7) corresponds to a low content of Ca and P. On the other hand, the marrow cavity is characterised by 4-times higher Fe concentrations than the bone material, explaining the relatively high <sup>226</sup>Ra concentrations by adsorption processes on the Fe hydroxides (Feige & Wiegand 1998). The surface

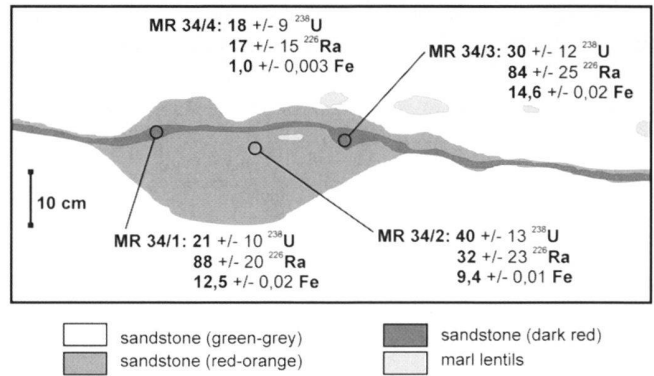


Fig. 3. <sup>238</sup>U, <sup>226</sup>Ra [Bq/kg] and Fe [wt-%] concentrations with  $2\sigma$  errors of samples from outcrop “military road”. Mt. Vully (sketch from a photograph).

bonding of adsorbed <sup>226</sup>Ra goes along with a high <sup>222</sup>Rn emanation, resulting in a large <sup>222</sup>Rn loss, and therefore in low <sup>210</sup>Pb concentrations.

In the course of the investigation, precipitations of Fe hydroxides were noticed frequently within sandstones of the transition zone between USM and OMM. The precipitations occur in structures like tubes, ribbons or nests. Some of them are characterised by higher contents of radionuclides, especially of <sup>226</sup>Ra. Fig. 3 shows an example of a ribbon like precipitation of Fe hydroxides from the Mt. Vully outcrop “military road”. The ordinary sandstone (MR 34/4) surrounding the precipitation carries glauconite, which results in colours between green to grey. The <sup>238</sup>U and <sup>226</sup>Ra concentrations of the sandstone are low and within a radioactive equilibrium. The region of the Fe precipitation has a higher content of organic material. It is divided into two parts, corresponding with the intensity of the reddish and brownish colours, and therefore with the Fe content. Parallel with an increase of Fe concentrations, the ones for <sup>226</sup>Ra increase as well, but remain more or less unchanged for <sup>238</sup>U.

##### 4.2 Les Dailles

At the large artificial excavation of Les Dailles, very striking radioactive disequilibria were observed, which are markedly different from those of Mt. Vully. The analysis of samples W 93/4 – W 93/6.1 (Tab. 2) were done by Surbeck (pers. communication). The two green to grey coloured sandstones W 93/4 and W 93/5 were sampled at the base of a channel, just above an impermeable marly bed. Both samples are characterised by a significant enrichment of <sup>238</sup>U, while the concentrations of <sup>226</sup>Ra and <sup>210</sup>Pb are noticeably lower, and within equilibrium conditions. A grain-size separation and subsequent analysis made by Surbeck (pers. communication) showed that most of the <sup>238</sup>U was localised in grains of a size < 63 µm.

From the same outcrop two fillings of a joint with high contents of Fe and Mn hydroxides were sampled (Tab. 2, W 93/6

and W 93/6.1), which show radioactive disequilibria contrasting to the two samples described above. While the  $^{238}\text{U}$  concentrations are below the detection limit, the samples are enriched in  $^{226}\text{Ra}$ . During a leaching process with oxalic acid-ammonium oxalate,  $^{226}\text{Ra}$  as well as the hydroxides were almost totally detached (Surbeck, pers. communication). The relatively low  $^{210}\text{Pb}$  concentrations emphasise the exposed position of  $^{226}\text{Ra}$  within the sample, indicating a high  $^{222}\text{Rn}$  emanation coefficient.

## 5. Discussion of radioactive disequilibria in sediments

It is very likely that the  $^{238}\text{U}$  enrichments within the sediments, which are documented by the samples with bone fragments (Tab. 2, W 93/1 – MR 9704), took place during early diagenetic times. Subsequently to the deposition of sand and organic material just above marly layers, oxidising ground waters with solute  $\text{U}^{6+}$  species (probably the  $\text{UO}_2(\text{HPO}_4)_2^{2-}$ ; Baertschi & Keil 1992) flowed through the sand. In the course of the microbiological degradation of organic material a strong reducing environment is developed (Schneider & Walther 1988). Here  $\text{U}^{6+}$  was reduced to  $\text{U}^{4+}$ , which led to the formation of little soluble U species, e.g.  $\text{U}(\text{OH})_4$  (Langmuir 1978). Furthermore,  $\text{Ca}^{2+}$  can be substituted by  $\text{U}^{4+}$  in apatite, which is a major component of bones (Abele & Salger 1962). For the development of the observed marked U enrichments it is not necessary to have high  $\text{U}^{6+}$  concentrations within the oxidising ground waters - average concentrations and a persistent supply are sufficient.

Most bone samples are close to radioactive equilibrium between  $^{238}\text{U}$  and  $^{226}\text{Ra}$  (Tab. 2), with the exception of the marrow cavity sample (MR 303/16.7) and sample MR 9704. Assuming that the early diagenetic enrichment of U took place as  $^{238}\text{U}$  and  $^{234}\text{U}$  precipitation (probably the latter in a larger part),  $^{226}\text{Ra}$  is starting to grow following the half-life of the intermediate  $^{230}\text{Th}$  (75000 years). Equilibrium conditions within the whole  $^{238}\text{U}$  series will be reached after approx. 1.5 million years (6 half-lives of  $^{234}\text{U}$ ). Considering a Tertiary U enrichment, the sediment samples should have achieved equilibrium conditions, if there was no other geo- or hydrochemical process active, affecting radionuclide mobility.

The Fe hydroxide precipitations of the outcrop "military road" at Mt. Vully with increased  $^{226}\text{Ra}$  concentrations (Fig. 3), show a corresponding distribution of Fe and organic material (Schott 1998). This indicates that the decomposition of the latter made the Fe precipitation possible. During the decomposition of the organic material, Fe hydroxides could be precipitated at the border zone between a reducing halo and an oxidising ground water. It is very likely that the Fe precipitations continued subsequent to the decomposition. Due to the decay of organic material the permeability of the sediment was enhanced, which supports a change from reducing to oxidising conditions, and therefore a precipitation of Fe hydroxides (Blume 1984). Probably, the glauconite served as the Fe source for the precipitations.

The radioactive disequilibria of the sandstones of Fig. 3 show two- or threefold enrichments of  $^{226}\text{Ra}$  (MR 34/1, MR 34/3). The  $^{210}\text{Pb}$  concentrations are below the detection limit (approx. 30 Bq/kg) with the exception of sample MR 34/3 ( $31 \pm 18$  Bq/kg). The disequilibrium was achieved rather by an enrichment of  $^{226}\text{Ra}$  than by a depletion of  $^{238}\text{U}$ . Fe and Mn hydroxides are well known for their high capability to adsorb Ra, especially when the hydroxides are freshly precipitated (Feige & Wiegand 1998; Wiegand 2001). The low  $^{210}\text{Pb}$  concentrations of the samples are evidence of a major  $^{222}\text{Rn}$  loss, which is explained by a high availability of  $^{222}\text{Rn}$  due to the exposed position of  $^{226}\text{Ra}$  within the sample. To verify this assumption,  $^{222}\text{Rn}$  emanation coefficients were analysed of four selected sandstone samples with different Fe concentrations. In agreement with the Fe content (1.2, 3.8, 5.4 and 12.5 wt-% Fe), the  $^{222}\text{Rn}$  emanation coefficient increases as well: 4, 13, 10 and 16 % (errors: 17, 7, 3.5 and 6 %). According to Korner & Rose (1977), the  $^{222}\text{Rn}$  emanation coefficient of sedimentary rocks averages at 9 % (including strong emanators like fine-grained clastic material), which underlines the high emanation coefficient of the coarse-grained Fe-rich sandstone samples. If such sediments occur in aquifers, the ground water should be characterised by a high content of  $^{222}\text{Rn}$ . Considering the half-life of  $^{226}\text{Ra}$  (1600 years), the Ra enrichment of the sediments must have taken place during the last 10000 years, i.e. the Holocene. Older enrichments are not recognisable any more due to the complete decay of excess  $^{226}\text{Ra}$ .

The source rock from which the excess  $^{226}\text{Ra}$  originates, must show a depletion of  $^{226}\text{Ra}$ . Such sediments are represented by the samples W 93/4 and W 93/5 (Tab. 2), which are characterised by high  $^{238}\text{U}$  and low  $^{226}\text{Ra}$  concentrations. Therefore, the four last samples of Tab. 2, which show two different radioactive disequilibria, can be explained as follows. Reducing ground waters mobilised Fe, Mn and  $^{226}\text{Ra}$  from some sediment parts (samples W 93/4 and W 93/5). When the ground water reached oxidising conditions, as are found along permeable faults and joints or permeable beds, Fe and Mn hydroxides were precipitated, and  $^{226}\text{Ra}$  was adsorbed on hydroxide surfaces (samples W 93/6 and W 93/6.1). Terminating the  $^{226}\text{Ra}$  supply, the radioactive disequilibrium will vanish after several 1000 years, indicating a subrecent  $^{226}\text{Ra}$  enrichment at Les Dailles. This is in accordance with the deep artificial excavation at the location, cutting into an active aquifer. In contrast to that, the natural outcrops at Mt. Vully now show little hydraulic activity, and the  $^{226}\text{Ra}$  enrichments of Fe hydroxide precipitations in sandstones have almost decayed.

## 6. Chemical classification of Mt. Vully ground waters

The ground waters of Mt. Vully have a chemical composition that is very similar to neighbouring ground waters from the OMM described by Hesske (1995). The main ions are Ca, Mg and  $\text{HCO}_3$  (average concentration: 107, 27 and 345 mg/l; Schott 1998). Following Davis & De Wiest (1967), all the analysed waters can be designated as Ca- $\text{HCO}_3$  waters, or as

Ca-Mg-HCO<sub>3</sub> waters, if the classification after Michel (1963) is used. The only exception is water catchment 25, where a Ca-Mg-HCO<sub>3</sub>-(Cl) water was sampled. This sample shows a fertiliser impact, indicated by relatively high concentrations of NO<sub>3</sub> (12 mg/l) respectively Cl (22 mg/l)

## 7. Radionuclide content of Mt. Vully ground waters

The main differences between the waters of the 25 catchments are found in their radionuclide composition, which are summarized in Fig. 4, and allowed a grouping of the catchments. The water catchments 1 and 2 (group 1) are located at the northern slope of Mt. Vully (Fig. 1). Only the water catchments of group 1 and 2 are former natural springs. All the other groups (3 – 7) represent one manhole, where ground water is collected by different drainage pipes. All ground waters originate from the OMM aquifer. Nevertheless it is very likely, that the ground waters of group 7 are influenced by morainic deposits to some degree.

### 7.1 <sup>238</sup>U, <sup>234</sup>U, <sup>226</sup>Ra

Most of the analysed waters are characterised by enhanced concentrations of non-gaseous radionuclides, in particular <sup>238</sup>U and <sup>234</sup>U. Ground waters from the OMM aquifer nearby the Mt. Vully analysed by Hesske (1995) have significantly lower U concentrations of 1.0 – 3.1 µg/l, which is equal to approx. 12 – 38 mBq/l <sup>238</sup>U at same <sup>238</sup>U / <sup>234</sup>U proportions. The <sup>238</sup>U and <sup>234</sup>U concentrations of waters from the investigated water catchments vary between 16 and 184 mBq/l and 53 – 219 mBq/l respectively, indicating a slight excess of <sup>234</sup>U, which, with exception of catchment 10, lies within the 2 σ measurement error (Fig. 4). Because of the oxidising conditions of the waters, the <sup>226</sup>Ra concentrations are clearly lower, and vary between 3 and 29 mBq/l. The largest variation of radionuclide concentrations is shown by <sup>222</sup>Rn, which ranges from 6 to 105 Bq/l, an order of magnitude higher than the non-gaseous radionuclides.

### 7.2 <sup>222</sup>Rn

While the discharge of the water catchments during the second sampling is higher than or at least equal to the first sampling, the <sup>222</sup>Rn concentrations are more or less the same with the exceptions of catchments 8 and 15 (Tab. 1, Fig. 4). In a first approximation the <sup>222</sup>Rn concentrations of the analysed waters show a similar distribution as the concentrations of the non-gaseous radionuclides (Fig. 4). The waters of group 3 (catchments 5, 6, 7) have relatively low <sup>222</sup>Rn concentrations (approx. 10 Bq/l). Especially the waters of group 1 and 2, as well as catchment 10 are characterised by high <sup>222</sup>Rn concentrations, reaching 100 Bq/l.

Following Kraemer & Reid (1984) and Wiegand (2001), <sup>222</sup>Rn can be transferred to the ground water by four different possibilities: First, dissolved <sup>226</sup>Ra can decay in the ground water. Considering that the <sup>222</sup>Rn concentration is an order of

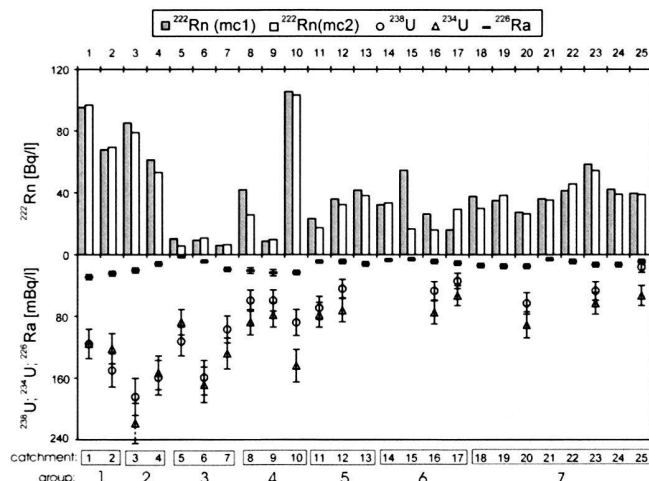


Fig. 4. <sup>222</sup>Rn concentrations of water (1 σ error: 8% for < 10 Bq/l, 4% for > 10 Bq/l) sampled during 2 measuring campaigns (mc 1, mc 2), and <sup>238</sup>U, <sup>234</sup>U and <sup>226</sup>Ra concentrations (with 2 σ error bars) from mc 1.

a magnitude higher than that of <sup>226</sup>Ra (Fig. 4), this possibility can be only of marginal importance. Second, <sup>222</sup>Rn bearing soil-gas or meteoric water can come into contact with ground water, a process which was observed by Surbeck & Eisenlohr (1995) in Swiss karst springs. This process can be dominant. Looking at the high <sup>222</sup>Rn concentrations of Mt. Vully's ground water, compared with the ones of the neighbouring regions with similar soils, the sedimentary rocks are more likely the source of <sup>222</sup>Rn than the soils. Third, a <sup>226</sup>Ra atom decays within a mineral grain close to the surface, and <sup>222</sup>Rn is catalypted by α-recoil direct into the ground water. This process depends on the distribution of <sup>226</sup>Ra within the mineral (Tanner 1980). Fourth and finally, <sup>222</sup>Rn is generated directly at the grain surface through the decay of <sup>226</sup>Ra, which is adsorbed on mineral grains. Especially the latter process should be of major importance for the Mt. Vully ground waters. Fe and Mn hydroxide precipitations were observed not only at the natural outcrop "military road" at Mt. Vully, but especially at the artificial excavation "Les Dailles".

## 8. Discussion of the radionuclide distribution in ground waters

A comparison of the radionuclide concentrations shows that the highest concentrations and the largest variations within and between groups are found for the first four groups (Fig. 4). The other three groups (water catchments 11 – 25) do not show much variation. Group 1 and group 2 are similar in their radionuclide composition, although their catchments are not neighbouring (Fig. 1). Among the 25 investigated water catchments, the catchments 1 – 4 are the only ones which do not collect ground water via long drainage pipes (Tab. 1), but capture spring waters. This is proven for catchments 1 and 2, and very likely for catchments 3 and 4, suggesting that the ground



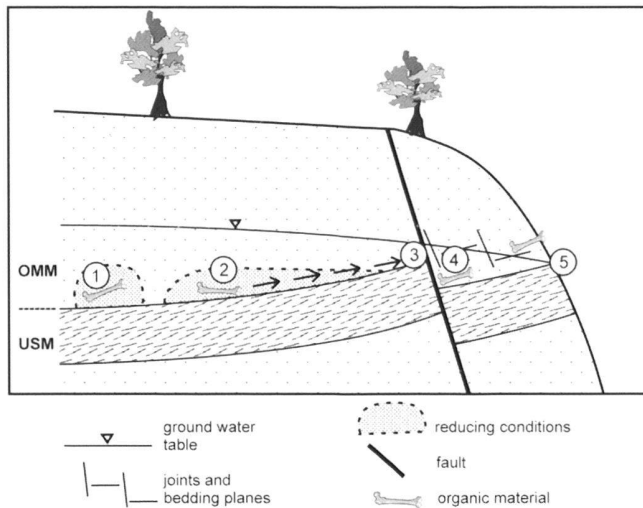


Fig. 5. Synoptical sketch of radionuclide enrichment, mobility and displacement at Mt. Vully and Les Dailles. The numbers indicate processes, which are explained in the text.

water of the four catchments originate from highly permeable regions, like faults or extensively jointed sandstones. Catchments 3 and 4 are very close to an assumed fault, which was mapped by Geolina (1993) (Fig. 1). The relatively high  $^{226}\text{Ra}$  concentrations of the water from the four catchments result from a mobilisation of  $^{226}\text{Ra}$ , which is adsorbed on Fe and Mn hydroxides along the faults. The mobilisation process can be explained by diffusion or ion exchange from the highly Ra-enriched hydroxides. The high concentrations of  $^{238}\text{U}$  and  $^{234}\text{U}$  in the waters can be traced back to the U-rich organic material in the lower parts of the aquifer.

The water of the three catchments of group 3 have a similar composition of non-gaseous radionuclides like the water from the first four catchments (Fig. 4) – the marked differences in  $^{222}\text{Rn}$  are discussed later. Due to the very long drainage pipes (95 m, Tab. 1), the source of the captured ground water is not well known, but it is believed to originate from the base of OMM, explaining the enhanced  $^{238}\text{U}$  and  $^{234}\text{U}$  concentrations. Within the fourth group (catchments 8 – 10) the  $^{226}\text{Ra}$  concentrations display relatively high levels (Fig. 4), indicating the vicinity of a  $^{226}\text{Ra}$  rich fault. Indeed, a fault mapped by Geolina (1993), is situated just north of catchment 10 (Fig. 1). Within group 4, catchment 10 is notable because of its enhanced  $^{238}\text{U}$  and  $^{234}\text{U}$  concentrations, and its striking excess of  $^{234}\text{U}$ . This disequilibrium points to surface-bound U atoms within the sediment, and therefore to a high availability of U. While  $^{238}\text{U}$  is fixed more strongly,  $^{234}\text{U}$  follows after the  $\alpha$ -decay of  $^{238}\text{U}$ , which can catapult the generated radionuclide ( $^{234}\text{Th}$ ) via  $\alpha$ -recoil into the ground water (Kigoshi 1971).

The variation of  $^{222}\text{Rn}$  concentrations is similar to the variation of the non-gaseous radionuclide concentrations (Fig. 4). Nevertheless, the length of drainage pipes modifies the  $^{222}\text{Rn}$

concentrations strongly. In particular, a comparison of the first three groups underlines the influence of the pipes. While the water catchments of the first two groups have no drainage pipes, ensuring that “fresh” spring water is sampled, catchments 5 – 7 are characterised by 95 m long drainage pipes (Tab. 1). Therefore, the water of the latter catchments are partly degassed during their long passage in unsaturated drainage pipes. This is supported by low  $\text{CO}_2$  concentrations of the water compared with the average of all water catchments (Schott 1998). Furthermore, the highest water temperatures were measured at water catchments 5 – 7 (Schott 1998), which is another indicator for a relatively long duration of the seepage. The highest  $^{222}\text{Rn}$  concentration among all 25 water catchments was measured at catchment 10 (105 Bq/l). This catchment collects ground water via a 25 m long drainage pipe (Tab. 1). As already mentioned, catchment 10 is in the vicinity of an assumed fault (Fig. 1). This situation, together with high  $^{226}\text{Ra}$  concentrations and a marked excess of  $^{234}\text{U}$  compared to  $^{238}\text{U}$  (Fig. 4), leads to the hypothesis that water percolates through a fault, which is mineralised with Fe and Mn hydroxide precipitations with adsorbed  $^{226}\text{Ra}$ . Since the drainage pipe is not too long (25 m), the high  $^{222}\text{Rn}$  emanation coefficient of such precipitations ensures high  $^{222}\text{Rn}$  concentrations in the water. Therefore, water catchments 1, 2, 3, 4 and 10 represent a very similar hydrogeological setting.

## 9. Conclusions

An investigation about gaseous and non-gaseous radionuclides within sediments and ground waters of an isolated aquifer in a small rainfall catchment area, suggests the following explanation for the establishment of different radionuclide enrichments and pathways. The processes are pictured and summarised with the help of a schematic cross section through the Mt. Vully (Fig. 5). For each process examples of analysed samples are given:

1. Deposition of coarse-grained clastic and organic material (alluvial wood, bones) in the transition zone of USM / OMM, and early diagenetic U precipitation at organic material due to the development of a reducing halo (e.g. sample MR 303/16.4.2).
2. Mobilisation of Fe, Mn and  $^{226}\text{Ra}$  under local reducing conditions, probably in the direct vicinity of the impermeable marly beds of USM (e.g. sample W 93/5). Subsequent transport of dissolved cations with the ground water stream.
3. Precipitation of Fe and Mn hydroxides under oxidising conditions, and adsorption of  $^{226}\text{Ra}$  on hydroxides (e.g. sample W 93/6).
4. U-rich organic material ( $^{238}\text{U}$ ,  $^{234}\text{U}$  and  $^{226}\text{Ra}$ ) within the aquifer under oxidising conditions (e.g. sample MR 303/16.4.2).
5. Ground water, which was  $^{238}\text{U}$ - and  $^{234}\text{U}$ -enriched at location (4), and  $^{226}\text{Ra}$ - and  $^{222}\text{Rn}$ -enriched at location (3), flows out at a spring (e.g. water catchment 1).

While the process (1) occurred during the Tertiary, the other processes are still going on today. At the natural outcrops and captured ground waters of Mt. Vully only process (5) and situation (4) were identified, but it is concluded that the other processes still take place in the depth of Mt. Vully. This is supported by the findings of the deep artificial excavation of Les Dailles, where an active aquifer was cut, and proofs for the remaining processes (2) and (3) were found.

## Acknowledgements

The paper benefited from the discussions with many colleagues. Special thanks are due to Heinz Surbeck, who initiated and accompanied this investigation. Most of the analyses were conducted under his direction, and he gave access to data, which were collected by him earlier. The paper benefited greatly from reviews by Edi Hoehn (Dübendorf) and an anonymous reviewer. The study was financially supported by the Swiss Federal Office of Public Health.

## REFERENCES

- ABELE, G. & SALGER, M. 1962: Die Uranvorkommen im Burgsandstein Mittelfrankens. Teil B: Zur Chemie und Mineralogie der Aktivarkosen. *Geologica Bavarica*, 49, 59–90.
- BADONE, E. & FAROUHAR, R.M. 1982: Application of neutron activation analysis to the study of elemental concentration and exchange in fossil bone. *J. Radioanal. Chem.*, 69 (1–2), 291–311.
- BAERTSCHI, P. & KEIL, R. 1992: Urangelhalte von Oberflächen-, Quell- und Grundwässern der Schweiz. NTB 91–26, NAGRA-Nationale Genossenschaft für die Lagerung radioaktiver Abfälle, Wettingen
- BECKER, F. 1973: Geologischer Atlas der Schweiz, 1:25 000. Notice explicative feuille Murten (1165).
- BECKER, F. & RAMSEYER, R. 1972: Geologischer Atlas der Schweiz, 1:25 000. Blatt Murten (1165).
- BLUME, H.-P. 1984: Bodenentwicklung, Bodensystematik und Bodenverbreitung. In: *Lehrbuch der Bodenkunde* (Ed. by BLUME, H.-P., HARTGE, K.H., SCHACHTSCHABEL, P., Schwertmann, U.). Enke Verlag, Stuttgart, 321–412.
- DAVIS, S.N. & DE WIEST, R.J.M. 1967: *Hydrogeology*. Wiley Verlag, New York-London-Sydney.
- EIDGENÖSSISCHES DEPARTEMENT DES INNERN 1995: Verordnung über Fremd- und Inhaltsstoffe in Lebensmitteln (Fremd- und Inhaltsstoffverordnung, FIV) vom 26. Juni 1995, Stand 22. Februar 2000.
- FEIGE, S. & WIEGAND, J. 1998: Einfluß des Kohlebergbaus auf das Radon-Potential. In: *Radioaktivität in Mensch und Umwelt* (Ed. by WINTER, M., HENRICH, K. & DOERFEL, H.). Publikationsreihe Fortschritte im Strahlenschutz Bd. II, 930–935.
- GEOLINA 1993: Dimensionnement des zones de protection "S" des captages de val Florenche & du Vailet. Unpubl. Rapport Hydrogéologique 93–133, Fribourg.
- HESSKE, S. 1995: Typologie des eaux souterraines de la Molasse entre Chambéry et Linz (France, Suisse, Allemagne, Autriche). Diss. École Polytech. Féd. Lausanne.
- HOMWOOD, P. & MATTER, A. 1980: Berne-Mt-Vully-Flue-Schwarzenburg-Fribourg. In: *Geology of Switzerland – a guide-book* (Ed. By TRÜMPY, R.). Part B, 287–289.
- KELLER, B. 1992: Hydrogeologie des schweizerischen Molasse-Beckens: Aktueller Wissensstand und weiterführende Betrachtungen. *Eclogae geol. Helv.* 85/3, 611–651.
- KIGOSHI, K. 1971: Alpha recoil Thorium-234: Dissolution into water and the uranium-234/uranium-238 disequilibrium in nature. *Science* 173, 47–48.
- KORNER, L.A. & ROSE, A.W. 1977: Radon in streams and ground waters of Pennsylvania as a guide to uranium deposits. U.S. Dept. of Energy Report GJO-1659–20.
- KRAEMER, T.F. & REID, D.F. 1984: The occurrence and behaviour of radium in saline formation water of the U.S. Gulf Coast region. *Isotope Geoscience*, 2, 153–174.
- LANGMUIR, D. 1978: Uranium solution-mineral equilibria at low temperatures with applications to sedimentary ore deposits. *Geochim. Cosmochim. Acta* 42, 547–569.
- MICHEL, G. 1963: Untersuchungen über die Tiefenlage der Grenze Süßwasser-Salzwasser im nördlichen Rheinland und anschließenden Teilen Westfalens, zugleich ein Beitrag zur Hydrologie und Chemie des tiefen Grundwassers. *Forsch.-Ber. Land NRW*, Nr. 1239
- RAMSEYER, R. 1952: Geologie des Wistenlacherberges (Mont Vully) und der Umgebung von Murten (Kt. Freiburg). *Eclogae geol. Helv.* 45/2, 165–217.
- SCHMID, S. & WIEGAND, J. 1998: The Influence of Traffic Vibrations on the Radon Potential. *Health Physics* 74 (2), 231–236.
- SCHNEIDER, H.-J. & WALTHER, H.W. 1988: Endlagerstätten in Sedimenten. In: *Sedimente und Sedimentgesteine* (Ed. by FÜCHTBAUER, H.). Schweizerbart'sche Verlagsbuchhandlung, Stuttgart, 569–682.
- SCHOTT, B. 1998: Geologische und hydrogeologische Untersuchungen zur Radionuklid-Mobilität am Mt. Vully (Canton Fribourg / Ch). Unpubl. diploma thesis, Univ. Essen, 124 p.
- SCHWARZ, H.P. & BLACKWELL, B.A. 1992: Archaeological Applications. In: *Uranium-series Disequilibrium: Applications to Earth, Marine, and Environmental Sciences* (Ed. by IVANOVICH, M. & HARMON, R.S.). Clarendon Press, 513–552.
- STUDER, B. 1853: *Geologie der Schweiz*. Stämpfli, Bern.
- SURBECK, H. 1991: Radium und Radon im Boden, messtechnische und geologische Aspekte. In: *Messung von Radon und Radon-Folgeprodukten* (Ed. by VÖLKLE, H. & BORCHARDT, D.). Publikationsreihe Fortschritte im Strahlenschutz, 132–142.
- 1995: Determination of natural radionuclides in drinking water; a tentative protocol. *The Science of the Total Environment* 173/174, 91–99.
  - 1997: Radon und Trinkwasser. In: *Schriftenreihe des Vereins für Wasser-, Boden- und Lufthygiene* (Ed. by AURAND, K. & RÜHLE, H.), 101, Berlin.
- SURBECK, H. & EISENLOHR, L. 1995: Radon as a natural tracer to study transport processes in a karst system. An example in the Swiss Jura. *C.R. Acad. Sci. Paris* 321, ser. II a, 761–767.
- TANNER, A.B. 1980: Radon migration in the ground: a supplementary review. In: *The natural radiation environment, III* (Ed. by GESELL, T.F. & LOWDER, W.M.). *Nat. Techn. Inform. Service*, U.S. Dept. of Energy Rep. CONF-780422, 5–56.
- UNSCEAR-UNITED NATIONS SCIENTIFIC COMMITTEE ON THE EFFECTS OF ATOMIC RADIATION 2000: Sources and Effects of Ionizing Radiation. Vol. 1, 654 p.
- VÖLKLE, H. & GOBET M. 1997: *Umweltradioaktivität und Strahlendosen in der Schweiz 1996* (Ed. by BAG-BUNDESAMT FÜR GESUNDHEIT). BAG, Bern.
- WIEGAND, J. 2001: A guideline for the evaluation of the radon potential based on geogenic and anthropogenic parameters. *Environmental Geology* 40, 949–963.

Manuscript received May 30, 2001

Revision accepted December 5, 2002

